engineering proceedings

Proceeding Paper

Preparation of Rotor Geometry for Setting up Numerical Model of Flow in Refining Ladle †

Lukáš Manoch [1,*], Ladislav Socha [2], Jana Sviželová [2], Karel Gryc [2] and Adnan Mohamed [2]

1 Department of Machine Designs, Faculty of Mechanical Engineering, University of West Bohemia, 301 00 Pilsen, Czech Republic
2 Environmental Research Department, Institute of Technology and Business in České Budějovice, 370 01 České Budějovice, Czech Republic; socha@mail.vstecb.cz (L.S.); gryc@mail.vstecb.cz (K.G.); mohamed@mail.vstecb.cz (A.M.)
* Correspondence: lmanoch@fst.zcu.cz; Tel.: +420-777-319-043

† Presented at the 30th International Conference on Modern Metallurgy—Iron and Steelmaking, Kosice, Slovakia, 27–29 September 2023.

Abstract: Foundry Degassing Units (FDU) are used for refining aluminum alloys. For an ideal refining process using an FDU unit, it is necessary to select several parameters, which are linked to each other. For a rotary impeller, we searched for several parameters, such as its optimal shape, speed in the liquid alloy, and distance from the bottom of the refining ladle, where the aforementioned parameters contribute to the overall wear and life of the rotor and, consequently, of the rotor shaft. The Computational Fluid Dynamics (CFD) method can be used to determine the above-mentioned parameters. This paper describes the particular steps of preparation of rotor geometry for the subsequent setting up of the basic numerical model.

Keywords: aluminum refining; FDU unit; 3D CAD; Computational Fluid Dynamics (CFD)

Citation: Manoch, L.; Socha, L.; Sviželová, J.; Gryc, K.; Mohamed, A. Preparation of Rotor Geometry for Setting up Numerical Model of Flow in Refining Ladle. *Eng. Proc.* **2024**, *64*, 13. https://doi.org/10.3390/engproc2024064013

Academic Editors: Branislav Buľko, Dana Baricová, Peter Demeter and Róbert Dzurňák

Published: 28 February 2024

1. Introduction

Foundry Degassing Unit (FDU) refining systems are largely used to refine aluminum alloys. This unit is an automated metal treatment system for the degassing (hydrogen removal) and the purification of aluminum alloys. The principle of refining consists in forcing an inert gas using the rotor into the bottom part of the pan. The rotor divides the inert gas into fine bubbles and mixes them with the molten mass. The turbulent flow ensures agitation of the molten mass; this accelerates hydrogen transport from the molten mass to the molten mass-bubble interface [1].

The refining process using an FDU unit can be divided into particular cycles with regard to the rotor lifetime. In case the material of the rotor system is graphite, the geometry of the rotary impeller changes with the increasing number of cycles due to external phenomena such as oxidation at higher temperatures and abrasion, which subsequently has an effect on the refining process [2]. We can identify purely negative effects such as the peeling-off of the rotor parts, which affects the purity of the aluminum–liquid alloy after the refining. A change in the geometry of the rotary impeller due to the increasing number of cycles can have both a negative and positive impact. The geometry of the rotary impeller is formed by external phenomena and, if the initial shape of the geometry is chosen correctly, the shape can be optimized by the refining process itself [3].

Foundry process research is nowadays carried out through physical and numerical modeling [4–10] and operational tests. The refining of aluminum melt is no exception. One approach to simulation of the refining process is to use numerical methods. The Computational Fluid Dynamics (CFD) method can describe not only the flow and pressure fields during the refining, but also the refining process itself [11–19]. The CFD method is also one of the options to verify whether the wear process of the rotor has a negative or a positive impact on degassing efficiency, or to perform the optimization of the rotary impeller shape itself. A necessary condition for the creation of the numerical model is the input geometry of the simulated part, which will be further discretized. The ideal scenario is to use the data from a physical experiment in order to validate the numerical simulation, and thus create a digital twin [20].

2. Basic FDU Geometry

The physical experiment, which will be the basis for future comparison with the numerical simulation, was equipped with regards to the baffle plate and the rotor system with identical components that are used on the FDU unit. Specifically, a rotor type A was used, consisting of a rotary impeller and a shaft, the parameters of which are presented in Table 1. The material of both components was graphite. The refining ladle was replaced by a container of a similar volume but made of a material allowing for monitoring the phenomena inside the refining ladle.

Table 1. Parameters of refining process and rotor design.

Rotor Type	Parameters of Refining Process		Rotor Design
A	Material Refining time Speed N flow rate Working height	Graphite 180 s 350 rpm 17 Nl·min^{-1} 160 mm	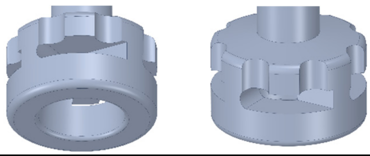

For the components in the basic state with zero cycles, no drawing documentation was available, and it was necessary to solve the conversion of real geometry to a 3D CAD model with regard to the components with a higher number of cycles. The need to create a 3D CAD model is not only due to obtaining data for numerical simulation, but also due to possible quantification of the loss of the rotor system.

Geometry of the Rotor System

The rotors were scanned with a high resolution using a ROMER Absolute Arm 7525SI device (with accuracy 0.05 mm) in order to obtain the data for the creation of 3D CAD geometry. The scan was subsequently exported in the form of a triangular mesh enabling further processing steps. The exported mesh format was STL format. (STL-Stereolithography).

Given the significant geometric complexity of the rotary impellers with multiple operating cycles, as shown in Figure 1a, it was necessary to develop a process for the input of triangular mesh in order to allow for the conversion to a 3D CAD model. Obtaining a 3D CAD model with the help of conventional methods of reverse engineering [21] was very complicated and time consuming. Maintaining the given level of detail, together with repeatability and speed were the conditions of the conversion process.

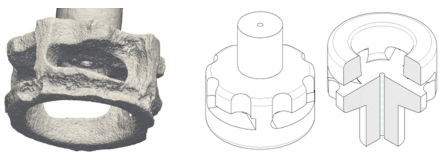

(**a**) (**b**)

Figure 1. Rotor type A geometry. (**a**) 1185 cycles, STL scan; (**b**) 0 cycles, 3D CAD.

The conversion process was divided into three separate steps:

1. Cleaning and simplifying the scanned data, defining the coordinate system, placing the geometry into a coordinate system. This step is identical for all rotors, regardless of the number of cycles;

2. Converting a triangular mesh to a purely square mesh;
3. Converting a square mesh to a 3D CAD model.

The exception to this were the rotor systems with zero cycles, as shown in Figure 1b, where only the first step of the entire process was used for the conversion, due to the clearly definable geometric elements. In this case, the conventional methods of reverse engineering could be used, and the input triangular mesh was used only as a reference for defining the position and dimensions of the extracted geometric elements.

In the first step of processing, it was crucial to create a watertight triangular mesh and its alignment to the required coordinate system. Creating the watertight triangular mesh consisted of removing any holes that were formed during the scanning process. The scanned data were positioned generally in space, and for further manipulation, it was necessary to align everything into a unified coordinate system. Regarding the fact that the entire rotor system was scanned as a whole, a clamping area was identified at the end of the rotor shaft that is outside the refining ladle area, as shown in Figure 2a. The connection of the rotary impeller and the rotor shaft was made by means of a bolted joint. For this type of connection, it is not possible to determine the same zero position for all rotary impellers. As a first processing step, the number of elements of the triangular mesh was reduced. A reduction of 40–50% had virtually no effect on the original shape of the mesh and significantly simplified the subsequent processing in the next step. The first processing step was the only processing step, which required an adjustment of the triangular mesh by the user.

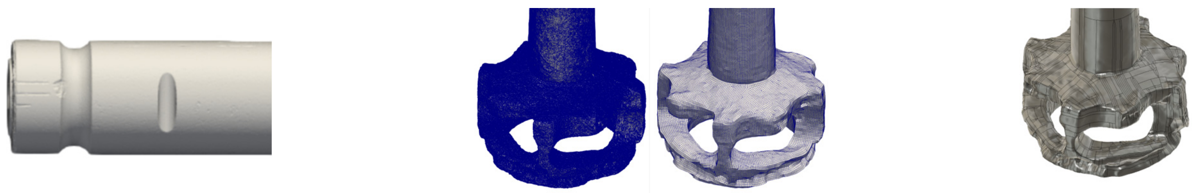

(**a**) (**b**) (**c**)

Figure 2. Rotor type A geometry. (**a**) Detail of clamping area of the rotor shaft used for unified alignment to the coordinate system; (**b**) 1185 cycles, original STL mesh (**left**), purely square mesh (**right**); (**c**) 3D CAD model, 1185 cycles.

The next step consisted of converting the triangular mesh to a purely square mesh. This completely automatic process only required defining the resultant number of elements of the square mesh. The number of elements was chosen mainly with regard to the use of geometry for the subsequent numerical simulation. Due to the expected character of the flow, the preservation of small details of the geometry would disproportionately increase the resultant number of elements of the computational mesh with a questionable effect on the resultant flow character. Repeatability for a particular scan while maintaining the same number of elements is 100%. The resultant resolution of the 3D CAD model is entirely dependent on the resolution of the purely square mesh.

The two above mentioned steps of the process, with regard to the possibilities of reduction, optimization, and remeshing of the input triangular mesh allow for adjustments in case of failure of the automatic conversions.

In the last step of the process, the square mesh was automatically converted to a 3D CAD model, as shown in Figure 2b. The result of the conversion to a 3D CAD model was the watertight element shown in Figure 2c, which was subsequently converted to a generic STEP format. As it was about the volume and not about the surface, it was possible to use the geometry for common volume operations, such as obtaining the total surface and total volume. Those values are not completely fundamental and necessary with regard to the future numerical simulation but allow to quantify the rotor loss depending on the number of operational cycles, for both high and low pressure regimes.

3. Results and Discussion

In case there is data for identical rotor systems with zero or more operational cycles, it is possible to use the particular 3D CAD models for obtaining data regarding the rotor material loss depending on the number of duty cycles, as shown in Table 2. The rotors were scanned at predefined intervals that corresponded to different stages of the lifespan (from 0 to 100%). The rotor material loss was evaluated in PolyWorks® 2021 IR9 software. The results do not consider all parameters, which were set on the FDU unit within the refining process; they take into account only the total number of cycles and the amount of loss on a given type of rotor system. For low (LP) and high pressure (HP) regimes, the rotor shaft has to be included in the total loss comparison.

Table 2. Quantification of material loss in the rotor system depending on operational cycles.

Rotor	Regime	Cycles	Shaft Volume (mm^3)	Rotor Volume (mm^3)	Loss of Material Shaft (%)	Loss of Material Rotor (%)
A	HP	0	3,637,275.947	2,030,257.657	0%	0%
	HP	739	2,907,731.577	693,206.579	20.06%	65.86%
	HP	936	3,524,843.212	876,099.357	3.09%	56.85%
	HP	1152	3,446,136.794	918,924.816	5.26%	54.74%
	HP	1185	3,364,399.409	791,155.046	7.50%	61.03%

Figure 3 shows the wear rate of rotor A at the end of its lifetime at 1185 cycles in the high-pressure regime. It can be observed that the wear of the rotary impeller at 1185 cycles is considerable and the level of the impact on the refining process is not negligible. From the geometry shape shown in Figure 3 it is evident that the rotary impeller shows a higher wear rate at the bottom of the geometry. The reason for this asymmetry may be due to the separation of the flow field in the refining ladle where this stimulus will be evaluated in the planned numerical simulation (CFD).

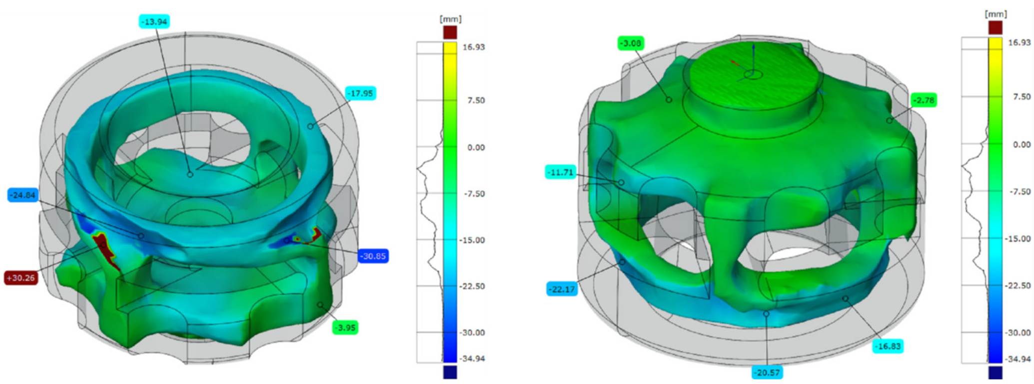

Figure 3. Rotor type A at 0 cycles (transparent geometry) at 1185 cycles.

4. Conclusions

A methodology of the conversion of complex scans of rotor systems into 3D CAD models for future use in numerical simulations (CFD) was developed. The methodology was validated and further used for quantification of the material loss in rotor systems depending on the number of operational cycles.

Author Contributions: Conceptualization, L.M.; methodology, L.M.; validation, L.M. and A.M.; formal analysis, L.M.; investigation, L.M. and A.M.; data curation, L.M. and A.M.; writing—original draft preparation, L.M.; writing—review and editing, J.S.; visualization, L.M.; supervision, L.S.; project administration, L.S. and K.G.; funding acquisition, L.S. All authors have read and agreed to the published version of the manuscript.

Funding: The paper was funded by the Technology Agency of the Czech Republic within the scope of the EPSILON program, as part of projects Reg. No. TH04010449 "Research and development of refining technologies for increasing of quality of aluminum alloys for high-performance quality castings".

Institutional Review Board Statement: Not applicable.

Informed Consent Statement: Not applicable.

Data Availability Statement: The raw data supporting the conclusions of this article will be made available by the authors on request.

Conflicts of Interest: The funders had no role in the design of the study; in the collection, analyses, or interpretation of data; in the writing of the manuscript; or in the decision to publish the results.

References

1. Myslivec, T. *Physico-Chemical Bases of Steel Industry*; SNTL: Prague, Czech Republic, 1971.
2. Prášil, T.; Socha, L.; Gryc, K.; Sviželová, J.; Saternus, M.; Merder, T.; Pieprzyca, J.; Gráf, M. Impact of Rotor Design on Its Wear and Work Efficiency of the Aluminum Refining Process. *Metals* **2022**, *12*, 1803. [CrossRef]
3. Socha, L.; Prášil, T.; Gryc, K.; Sviželová, J.; Saternus, M.; Merder, T.; Pieprzyca, J.; Nuska, P. Research on the impact of rotor wear on the effectiveness of the aluminium refining process. *Sci. Rep.* **2023**, *13*, 17758. [CrossRef] [PubMed]
4. Bul'ko, B.; Molnár, M.; Demeter, P. Physical Modeling of Different Configurations of a Tundish for Casting Grades of Steel that Must Satisfy Stringent Requirements on Quality. *Metallurgist* **2014**, *57*, 976–980. [CrossRef]
5. Bul'ko, B.; Molnár, M.; Demeter, P.; Baricová, D.; Pribulová, A.; Futáš, P. Study of the Influence of Intermix Conditions on Steel Cleanliness. *Metals* **2018**, *8*, 852. [CrossRef]
6. Rega, V.; Molnár, M.; Jusko, M.; Bul'ko, B.; Kijac, J.; Demeter, P. Impact of cast speed on the occurrence of the non-metallic inclusions in steel. *Acta Metall. Slovaca* **2016**, *22*, 4–13. [CrossRef]
7. Molnár, M.; Tréfa, G.; Hertneky, S.; Beháň, B.; Steranka, E.; Rega, V.; Jusko, M.; Legemza, J.; Bul'ko, B.; Demeter, P. Influence of chemical reheating at rh degasser on cleanliness of if steel grades. *Acta Metall. Slovaca* **2016**, *22*, 95–101. [CrossRef]
8. Baricová, D.; Pribulová, A.; Futáš, P.; Bul'ko, B.; Demeter, P. Change of the Chemical and Mineralogical Composition of the Slag during Oxygen Blowing in the Oxygen Converter Process. *Metals* **2018**, *8*, 844. [CrossRef]
9. Cao, Q.; Nastac, L. Mathematical Modeling of the Multiphase Flow and Mixing Phenomena in a Gas-Stirred Ladle: The Effect of Bubble Expansion. *JOM* **2018**, *70*, 2071–2081. [CrossRef]
10. Abreu-López, D.; Amaro-Villeda, A.; Acosta-González, F.A.; González-Rivera, C.; Ramírez-Argáez, M.A. Effect of the Impeller Design on Degasification Kinetics Using the Impeller Injector Technique Assisted by Mathematical Modeling. *Metals* **2017**, *7*, 132. [CrossRef]
11. Kuglin, K.; Szucki, M.; Pieprzyca, J.; Genthe, S.; Merder, T.; Kalisz, D. Physical and Numerical Modeling of the Impeller Construction Impact on the Aluminum Degassing Process. *Materials* **2022**, *15*, 5273. [CrossRef] [PubMed]
12. Saternus, M.; Merder, T. Numerical and Physical Modelling of Aluminium Refining Process Conducted in URO-200 Reactor. *Solid State Phenom.* **2012**, *191*, 3–12. [CrossRef]
13. Gómez, E.R.; Zenit, R.; Rivera, C.G.; Trápaga, G.; Ramírez-Argáez, M.A. Mathematical Modeling of Fluid Flow in a Water Physical Model of an Aluminum Degassing Ladle Equipped with an Impeller-Injector. *Metall. Mater. Trans. B* **2013**, *44*, 423–435. [CrossRef]
14. Sviželová, J.; Tkadlečková, M.; Michalek, K.; Walek, J.; Saternus, M.; Pieprzyca, J.; Merder, T. Numerical Modelling of Metal Melt Refining Process in Ladle with Rotating Impeller and Breakwaters. *Arch. Metall. Mater.* **2019**, *64*, 654–664. [CrossRef]
15. Yamamoto, T.; Suzuki, A.; Komarov, S.V.; Ishiwata, Y. Investigation of impeller design and flow structures in mechanical stirring of molten aluminum. *J. Mat. Process. Technol.* **2018**, *261*, 164–172. [CrossRef]
16. Maldonado, L.; Barron, M.; Miranda, D. Nitrogen Injection in Molten Aluminum in a Tank Degasser. *World J. Eng. Technol.* **2018**, *6*, 685–695. [CrossRef]
17. Abreu-López, D.; Dutta, A.; Camacho-Martínez, J.L.; Trápaga-Martínez, G.; Ramírez-Argáez, M.A. Mass Transfer Study of a Batch Aluminum Degassing Ladle with Multiple Designs of Rotating Impellers. *JOM* **2018**, *70*, 2958–2967. [CrossRef]
18. Warke, V.S.; Tryggvason, G.; Makhlouf, M.M. Mathematical modeling and computer simulation of molten metal cleansing by the rotating impeller degasser: Part I. Fluid flow. *J. Mater. Proces. Technol.* **2005**, *168*, 112–118. [CrossRef]
19. Wan, B.; Chen, W.; Mao, M.; Fu, Z.; Zhu, D. Numerical simulation of a stirring purifying technology for aluminum melt. *J. Mat. Process. Technol.* **2018**, *251*, 330–342. [CrossRef]

20. Grieves, M.A.; Vickers, J. Digital Twin: Mitigating Unpredictable, Undesirable Emergent Behavior in Complex Systems. In *Transdisciplinary Perspectives on Complex Systems*; Kahlen, F.J., Flumerfelt, S., Alves, A., Eds.; Springer: Cham, Switzerland, 2017; pp. 85–113.
21. Curtis, S.K.; Mattson, C.A.; Harston, S.P. On Barriers to Reverse Engineering Mechanical Components. In Proceedings of the ASME International Design Engineering Technical Conferences and Computers and Information in Engineering Conference, Montreal, QC, Canada, 15–18 August 2010; Volume 5.